

Kinetic Study of the Reactions of Chlorine Atoms and $\text{Cl}_2^{\bullet-}$ Radical Anions in Aqueous Solutions. 1. Reaction with Benzene

María L. Alegre, Mariana Geronés, Janina A. Rosso, Sonia G. Bertolotti,[†] André M. Braun,[‡] Daniel O. Mártire,* and Mónica C. Gonzalez*

Instituto de Investigaciones Fisicoquímicas Teóricas y Aplicadas (INIFTA), Facultad de Ciencias Exactas, Universidad Nacional de La Plata, Casilla de Correo 16, Sucursal 4, (1900) La Plata, Argentina

Received: August 23, 1999; In Final Form: December 16, 1999

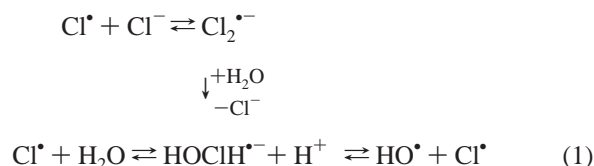
The photolysis of $\text{Na}_2\text{S}_2\text{O}_8$ aqueous solutions containing Cl^- ions is a clean method for kinetic studies of the species $\text{Cl}^\bullet/\text{Cl}_2^{\bullet-}$ in the absence and presence of added aromatic substrates. Laser and conventional flash-photolysis techniques were employed to investigate the aqueous phase reactions of chlorine atoms and $\text{Cl}_2^{\bullet-}$ (340 nm) radical ions in the presence and absence of benzene. A mechanism is proposed which accounts for the decay of $\text{Cl}_2^{\bullet-}$ in aqueous solutions containing chloride ion concentrations in the range 1×10^{-4} to 0.6 M, total radical ($\text{Cl}^\bullet + \text{Cl}_2^{\bullet-}$) concentrations in the range $(0.1-1.5) \times 10^{-5}$ M, and pH in the range 2.5–3.0. Interpretation of the experimental data is supported by kinetic computer simulations. The rate constants $6 \times 10^9 \text{ M}^{-1} \text{ s}^{-1} \leq k \leq 1.2 \times 10^{10} \text{ M}^{-1} \text{ s}^{-1}$ and $< 1 \times 10^5 \text{ M}^{-1} \text{ s}^{-1}$ were determined for the reactions of Cl^\bullet and $\text{Cl}_2^{\bullet-}$ with benzene, respectively, in the aqueous phase. The organic radicals produced from these reactions exhibit an absorption band with maximum at 300 nm, which was assigned to a Cl-cyclohexadienyl radical (Cl-CHD). The kinetic analysis of the traces supports a reversible reaction between O_2 and Cl-CHD. A reaction mechanism leading to the formation of chlorobenzene is proposed.

Introduction

Chloride is one of the most abundant anions in the tropospheric aqueous phase. In marine clouds, typical concentrations are in the order of 0.5 mM and higher concentrations can be found in aerosols.¹ HO^\bullet and $\text{SO}_4^{\bullet-}$ radicals, also present in cloud droplets and aerosols, have been reported to react with chloride ions yielding chlorine atoms, which are in equilibrium with $\text{Cl}_2^{\bullet-}$ radical ions.^{2,3} It is now apparent that reactions involving nitrogen oxide species and NaCl yielding chlorine atoms may also occur.^{1c} Therefore, oxidation of chloride may represent an important sink of strong oxidants in tropospheric multiphase systems, depending on the final fate of the Cl^\bullet atoms and $\text{Cl}_2^{\bullet-}$ radicals. In the marine scenario, the importance of the chemistry of the halogen atoms was suggested to be comparable to that of the HO^\bullet radical.

Reported rate constants of the reactions of $\text{Cl}_2^{\bullet-}$ indicate that this radical ion may have a lifetime of the order of fractions of milliseconds in tropospheric aqueous phase of low pH and high Cl^- concentrations.⁴ Therefore, reactions with organic and inorganic constituents of tropospheric droplets and aerosols may be important sinks for $\text{Cl}_2^{\bullet-}$. In contrast, due to the fast Cl^\bullet reaction with water, a lifetime of less than 5 μs was estimated for chlorine atoms under tropospheric conditions. Under such conditions, reactions of Cl^\bullet atoms with organic and inorganic compounds in the tropospheric aqueous phase should be negligible.^{5,6} However, the reactions of Cl^\bullet and $\text{Cl}_2^{\bullet-}$ with water were reported to involve a series of not well-established equilibria leading to the final formation of hydroxyl radicals,

as shown in eq 1. The detailed mechanism is still under discussion,^{2,7} because it cannot account for the observed experimental dependence of the $\text{Cl}_2^{\bullet-}$ decay on Cl^- concentration. Therefore, aqueous phase reactions of Cl^\bullet and $\text{Cl}_2^{\bullet-}$ need further investigations before Cl^\bullet reactions with constituents of the troposphere may be safely neglected.



Cl^\bullet and $\text{Cl}_2^{\bullet-}$ radicals are strong oxidants ($E(\text{Cl}_2^{\bullet-}/2\text{Cl}^-) = 2.0$ V and $E(\text{Cl}^\bullet/\text{Cl}^-) = 2.4$ V vs NHE)^{8,9} and may react with organic compounds by electron transfer, addition to double bonds and H-abstraction, with rates depending on the difference of the redox potentials.¹⁰

Aromatic compounds are important constituents of automotive gasoline and contribute to the formation of ozone and secondary organic aerosols. Our understanding of the atmospheric chemistry of aromatic compounds is incomplete, and assessments of the environmental impact of the release of such species are uncertain.¹¹ The determination of the reactivity of Cl^\bullet and $\text{Cl}_2^{\bullet-}$ radicals toward aromatic compounds is of environmental importance, as these reactions may lead to the formation of undesired chlorinated aromatic derivatives or else promote their oxidation.

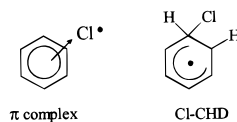
The reaction of chlorine atom with benzene in organic solvents has been interpreted to proceed via one or both of the intermediates (Chart 1) to explain the experimental results:^{12,13} a π complex and the 6-chlorocyclohexadienyl radical (Cl-CHD). The relation between these two species is not well-established, as related investigations present difficulties in

* To whom correspondence should be addressed. E-mail: dmartire@volta.ing.unlp.edu.ar. gonzalez@inifta.unlp.edu.ar. Fax: 54 221 425 4642.

[†] Universidad Nacional de Río Cuarto, Córdoba, Argentina.

[‡] Lehrstuhl für Umweltmesstechnik, Universität Karlsruhe, D-76128 Karlsruhe, Germany.

CHART 1



extracting information from systems equilibrating at rates which compete with bimolecular reactions.

An equilibrium between Cl^\bullet , C_6H_6 , and the intermediates was suggested, with an equilibrium constant $<10^3 \text{ M}^{-1}$.^{13,14} Absorption bands centered at 490 and 320 nm were observed, the first exhibiting a lifetime of 1 to 10 μs , was attributed to the π complex.^{12,14} On the basis of these observations, a mechanism was suggested involving the conversion of the π complex to the Cl-CHD radical.¹⁴ Because both absorbances remained independent of reaction temperature, other authors favored the existence of only the π complex intermediate.¹² However, investigations on the role of the Cl^\bullet -benzene complex in enhancing the selectivity of alkane photochlorinations favor the formation of the Cl-CHD radical. The hypothesis of a Cl-CHD intermediate is also supported by the formation of chlorobenzene as a reaction product.^{13a} Moreover, attempts to correlate the energy of the UV and visible absorption bands of a series of Cl^\bullet /arene complexes with the vertical ionization potentials and basicities of the arenes investigated failed to indicate a σ or π nature of the complex.¹⁵

The gas-phase reaction between Cl^\bullet atoms and benzene proceeds via H-atom abstraction and adduct formation.¹⁶ The equilibrium between Cl^\bullet atoms, benzene, and the intermediate strongly shifted toward the reactants, precludes the detection of the intermediate, for which a chlorocyclohexadienyl radical structure was proposed.

Despite the long history of the reaction of Cl^\bullet atoms with benzene, the nature of the main reaction channels is still not resolved. Moreover, this reaction has apparently never been investigated in the aqueous phase.

In this paper, we report a kinetic and mechanistic study on the aqueous phase reactions of $\text{Cl}_2^{\bullet-}$ and Cl^\bullet radicals and their reaction with benzene. This work is intended to contribute to the quantification of the aqueous phase atmospheric chemistry and to a better evaluation of the importance of $\text{Cl}_2^{\bullet-}$ and Cl^\bullet radicals in multiphase tropospheric chemistry.¹

Photolysis of $\text{S}_2\text{O}_8^{2-}$ ($\lambda_{\text{exc}} < 300 \text{ nm}$), reaction 1 in Table 1, is a clean source of sulfate radical ions with high pH-independent quantum yields.¹⁷ In the presence of Cl^- ions, reaction 2 has been reported to yield Cl^\bullet atoms, which reversibly react with Cl^- to yield $\text{Cl}_2^{\bullet-}$ radical ions, reactions 3 and 4.² The reactions of Cl^\bullet and $\text{Cl}_2^{\bullet-}$ are studied by laser and conventional flash-photolysis as well as by steady-state photolysis of $\text{S}_2\text{O}_8^{2-}$ solutions containing variable concentrations of Cl^- in the presence and absence of benzene.

Results and Discussion

Cl^\bullet and $\text{Cl}_2^{\bullet-}$ Reactions in Aqueous Solutions in the Absence of Benzene. Photolysis of aqueous peroxodisulfate solutions in the pH range of 2–3 showed formation of a transient species in the wavelength range from 300 to 550 nm whose decay rate and spectrum are in agreement with that reported in the literature for $\text{SO}_4^{\bullet-}$ radical ions in a wider pH range.^{17,18}

During irradiation experiments with chloride ion concentrations $[\text{Cl}^-]$ in the range of $1 \times 10^{-4} \text{ M}$ to 0.6 M, $\text{SO}_4^{\bullet-}$ radicals are readily depleted due to the high efficiency of reaction 2 yielding chlorine atoms. Reaction of Cl^\bullet with Cl^- ions reversibly yields $\text{Cl}_2^{\bullet-}$ radical ions, reactions 3 and 4. At $[\text{Cl}^-]$ used in

TABLE 1: Manifold of Reactions of Cl^\bullet and $\text{Cl}_2^{\bullet-}$ in Aqueous Solutions

	$k/\text{M}^{-1} \text{ s}^{-1} a$	
$\text{S}_2\text{O}_8^{2-} + h\nu \rightarrow 2 \text{SO}_4^{\bullet-}$		(1)
$\text{SO}_4^{\bullet-} + \text{Cl}^- \rightarrow \text{SO}_4^{2-} + \text{Cl}^\bullet$	$\log k = 8.43 + 1.0^{18} I^{1/2} b$	(2)
$\text{Cl}^\bullet + \text{Cl}^- \rightarrow \text{Cl}_2^{\bullet-}$	$8.5 \times 10^9 d$	(3)
$\text{Cl}_2^{\bullet-} \rightarrow \text{Cl}^\bullet + \text{Cl}^-$	$6.0 \times 10^4 \text{ s}^{-1} b$	(4)
$\text{Cl}_2^{\bullet-} + \text{Cl}_2^{\bullet-} \rightarrow \text{Cl}_2 + 2\text{Cl}^-$	$\log k = 8.8 + 1.6 I^{1/2} / (I^{1/2} + 1)^c$	(5)
$\text{Cl}_2^{\bullet-} + \text{HO}^- \rightarrow \text{ClOH}^{\bullet-} + \text{Cl}^-$	$4 \times 10^6 i$	(6)
$\text{Cl}_2^{\bullet-} + \text{H}_2\text{O} \rightarrow (\text{HOClH})^\bullet + \text{Cl}^-$	$1300 \text{ s}^{-1} b, d$	(7)
$\text{Cl}^\bullet + \text{H}_2\text{O} \rightarrow (\text{HOClH})^\bullet$	$2.5 \times 10^5 \text{ s}^{-1} b, d$	(8)
$(\text{HOClH})^\bullet \rightarrow \text{Cl}^\bullet + \text{H}_2\text{O}$	$(5 \pm 2) \times 10^4 \text{ s}^{-1} k$	(9)
$(\text{HOClH})^\bullet \rightarrow \text{ClOH}^{\bullet-} + \text{H}^+$	$1.0 \times 10^8 \text{ s}^{-1} b$	(10)
$\text{ClOH}^{\bullet-} + \text{H}^+ \rightarrow (\text{HOClH})^\bullet$	$3.0 \times 10^{10} e$	(11)
$\text{ClOH}^{\bullet-} \rightarrow \text{HO}^\bullet + \text{Cl}^-$	$6.1 \times 10^9 \text{ s}^{-1} e$	(12)
$\text{HO}^\bullet + \text{Cl}^- \rightarrow \text{ClOH}^{\bullet-}$	$4.3 \times 10^9 e$	(13)
$(\text{HOClH})^\bullet + \text{Cl}^- \rightarrow \text{Cl}_2^{\bullet-} + \text{H}_2\text{O}$	$(8 \pm 2) \times 10^9 l$	(14)
$\text{Cl}_2 + \text{H}_2\text{O} \rightarrow \text{ClOH} + \text{Cl}^- + \text{H}^+$	$11.0 \text{ s}^{-1} b$	(15)
$\text{Cl}_2 + \text{Cl}^- \rightleftharpoons \text{Cl}_3^-$	$K = 0.18 \text{ M}^{-1} h$	(16)
$\text{SO}_4^{\bullet-} + \text{S}_2\text{O}_8^{2-} \rightarrow \text{SO}_4^{2-} + \text{S}_2\text{O}_8^{\bullet-}$	$1.2 \times 10^5 g$	(17)
$\text{SO}_4^{2-} + \text{HO}^\bullet \rightarrow \text{SO}_4^{\bullet-} + \text{HO}^-$	$1.0 \times 10^6 f$	(18)
$\text{S}_2\text{O}_8^{2-} + \text{HO}^\bullet \rightarrow$	$<10^6 f$	(19)

^a Unless otherwise indicated. ^b Reference 2. ^c This work, in agreement with ref 2 at zero ionic strength. ^d Reference 7. ^e Reference 3. ^f Reference 32. ^g Reference 26. ^h Reference 25. ⁱ Reference 4. ^k This work. The program sensitivity to these rate constants is of the order of 10%. However, a larger dispersion is observed from the values required for the simulation of different experiments. ^l This work, in agreement with the value proposed in ref 2.

the present study, we may assume that equilibrium conditions are attained for reactions 3 and 4 (vide infra). Taking a value of $K_{3,4} = 1.4 \times 10^5 \text{ M}^{-1}$ for the stability constant,⁷ a ratio $[\text{Cl}_2^{\bullet-}]/[\text{Cl}^\bullet] > 10$ is expected for experiments with $[\text{Cl}^-] \geq 1 \times 10^{-4} \text{ M}$. Consequently, any contribution of chlorine atoms to the observed absorption traces can be neglected. Under the conditions of the time-resolved experiments, a transient species with an absorption maximum at $\lambda \sim 340 \text{ nm}$, whose spectrum agrees with that of $\text{Cl}_2^{\bullet-}$ radical ions is observed.¹⁹ The transient decay follows a complex kinetics strongly depending on $[\text{Cl}^-]$, as shown in Figure 1.

The transient absorbance profiles at a given wavelength, $A(\lambda, t)$, may be well fitted over more than three lifetimes with simultaneous first and second-order processes, according to eq 2.

$$A(\lambda, t) = \frac{ae^{-at}}{c(\lambda) - b(\lambda)e^{-at}} + d(\lambda) \quad (2)$$

where all the terms in the equation are highly sensitive to the chloride ion concentration. The constant a is independent of the detection wavelength λ while all other terms are wavelength dependent. Terms a and $b(\lambda)$ are related to the rate constants of the first and second-order decay processes, respectively. They are, within experimental error, independent of the presence of molecular oxygen and on the concentration of $\text{S}_2\text{O}_8^{2-}$. Terms $c(\lambda)$ and $d(\lambda)$ are related to the concentration of $\text{Cl}_2^{\bullet-}$, formed immediately after excitation and to the absorption of a longer lived species formed after $\text{Cl}_2^{\bullet-}$ depletion, respectively. Both $c(\lambda)$ and $d(\lambda)$ are highly sensitive to the irradiance and, in general, $d(\lambda) \ll c(\lambda)$.

The relative contribution of the first- and second-order decay processes strongly depends on $[\text{Cl}^-]$ and on the irradiance. In experiments with $[\text{Cl}^-] > 0.2 \text{ M}$, the dichloride radical ion was observed to decay mainly by a second-order process on the

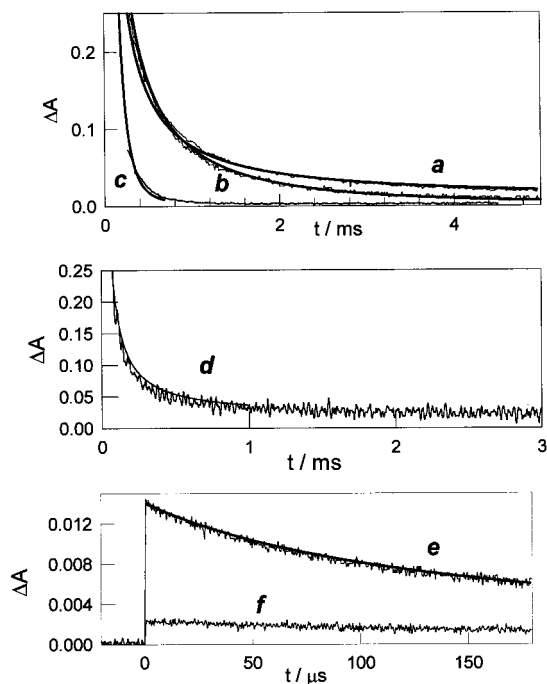


Figure 1. Absorption profiles at $\lambda_{\text{anal}} = 340$ nm obtained by conventional flash photolysis of 5×10^{-3} M $\text{K}_2\text{S}_2\text{O}_8$ solutions in the presence of different $[\text{Cl}^-]$: (a) 0.1 M, (b) 1×10^{-3} M and (c) 1×10^{-4} M, and (d) 0.6 M. Traces e and f correspond to absorption profiles following laser flash photolysis ($\lambda_{\text{exc}} = 266$ nm) of 2.25×10^{-2} M $\text{K}_2\text{S}_2\text{O}_8$ solutions in the presence of (e) 0.098 M Cl^- and $\lambda_{\text{anal}} = 340$ nm; (f) 0 M Cl^- and $\lambda_{\text{anal}} = 450$ nm. Solid curves represent computer simulations (refer to text).

millisecond time scale, as shown in Figure 1d for experiments with $[\text{Cl}^-] = 0.6$ M. In these experiments, almost no first-order component is observed within experimental error, even for very low initial concentrations of $\text{Cl}_2^{\bullet-}$.

The second-order component may be associated with the bimolecular decay of $\text{Cl}_2^{\bullet-}$ radical ions yielding Cl_2 and Cl^- ,^{2,20} reaction 5 in Table 1. Term $b(\lambda)$ is related to the rate constant k_5 by the expression $b(\lambda) = 2k_5/\epsilon(\text{Cl}_2^{\bullet-})_i$, where the optical path length l is 20 cm for conventional flash and 1 cm for laser experiments. The high sensitivity of $b(\lambda)$ to $[\text{Cl}^-]$ may be attributed to a real dependence on the ionic strength. The dependence of k_5 on the ionic strength (I), depicted in Figure 2, is consistent with the Debye–Hückel equation for a reaction between two single charged negative ions, eq 3.

$$\log k_5 = \log k_5^0 + 2 \frac{A\sqrt{I}}{1 + \sqrt{I}} \quad (3)$$

where k_5^0 stands for the rate constant at zero ionic strength, and A is a function of the temperature and physical constants of the solvent. Though this equation is strictly valid only at very low ionic strength, it holds reasonably well up to ionic strength values of 0.5 M, as also observed for the reactions of $\text{SO}_4^{\bullet-}$ with Cl^- .^{21,22} Although the observed value $A = 0.8$ is higher than the accepted value of 0.55 for water at 25 °C, extrapolation to infinite dilution leads to a rate constant $k_5^0 = 6.1 \times 10^8 \text{ M}^{-1} \text{ s}^{-1}$. The data reported in ref 2 for the ionic strength dependence of k_5 fall in the straight line shown in Figure 2.

The first-order rate coefficient of the $\text{Cl}_2^{\bullet-}$ decay markedly increases for $[\text{Cl}^-] < 10^{-3}$ M, a lower limit being found for $[\text{Cl}^-] > 0.1$ M, as illustrated in Figure 2 (inset). The observed tendency corroborates with the results reported by McElroy.²

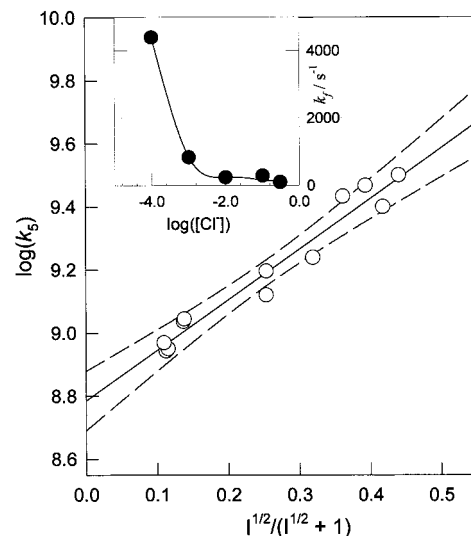


Figure 2. Dependence of the logarithm of the recombination rate constant k_5 on the ionic strength. Corresponding linear regression parameters are ordinate = 8.8, slope = 1.6, $r^2 = 0.94$. Dotted curves show the 99% confidence interval. Inset: First-order rate coefficient for the loss of $\text{Cl}_2^{\bullet-}$ as a function of $[\text{Cl}^-]$.

A mechanism involving reactions 3 and 4 and those of Cl^\bullet and $\text{Cl}_2^{\bullet-}$ with water, shown in eq 1, has been proposed for explaining the apparent first-order component of the $\text{Cl}_2^{\bullet-}$ decay and its dependence on $[\text{H}^+]$ and $[\text{Cl}^-]$.^{2,3,6,7} Any contribution of a reaction of Cl^\bullet and $\text{Cl}_2^{\bullet-}$ with peroxodisulfate is neglected, as no dependence of the first-order decay component on peroxodisulfate concentration is observed, in agreement with literature reports.^{7b} According to the mechanism shown in eq 1, reaction of Cl^\bullet and $\text{Cl}_2^{\bullet-}$ with water involves a series of equilibria leading to the final formation of chloride ions and HO^\bullet radicals. It may therefore be expected that further reactions removing HO^\bullet radicals would severely affect the equilibrium condition in eq 1, and the first-order decay component should depend on the rate of such reactions. When HO^\bullet radicals are completely removed, no equilibrium is established and reactions of Cl^\bullet and $\text{Cl}_2^{\bullet-}$ with water follow simple first-order kinetics, as observed by Buxton et al.⁷ Possible reactions removing HO^\bullet radicals in our reaction system are recombination and reactions with $\text{S}_2\text{O}_8^{2-}$ and SO_4^{2-} ions, reactions 18 and 19 in Table 1, respectively.

The kinetic analysis being rather complex, a computer program based on the numerical resolution of the differential equations system by the third-order Runge Kutta method was used in order to simulate the decay of the transient traces.^{23a} Stepsizes of the order of 10^{-10} – 10^{-9} s (depending on the experimental conditions) were checked for convergence and fixed throughout the complete simulation of a decay trace. The ability of the program to solve the system of differential equations was checked with a stiff solver method.^{23b} The program considers the pulsed excitation as a delta function, producing $\text{SO}_4^{\bullet-}$ radicals. The concentration of $\text{SO}_4^{\bullet-}$ present immediately after excitation $[\text{SO}_4^{\bullet-}]_0$ was taken as an input parameter, estimated from experiments under identical experimental conditions, but in the absence of Cl^- , as shown in Figure 1 for experiments e and f. Typical $[\text{SO}_4^{\bullet-}]_0$ values were of the order of $(2-3) \times 10^{-5}$ M and $(2-3) \times 10^{-6}$ M for experiments performed with conventional and laser flash techniques, respectively.

The program incorporates a set of well-established reactions involving the species present in the irradiated system, reactions 2–8 and 15–19, recombination of HO^\bullet radicals to yield H_2O_2 ,

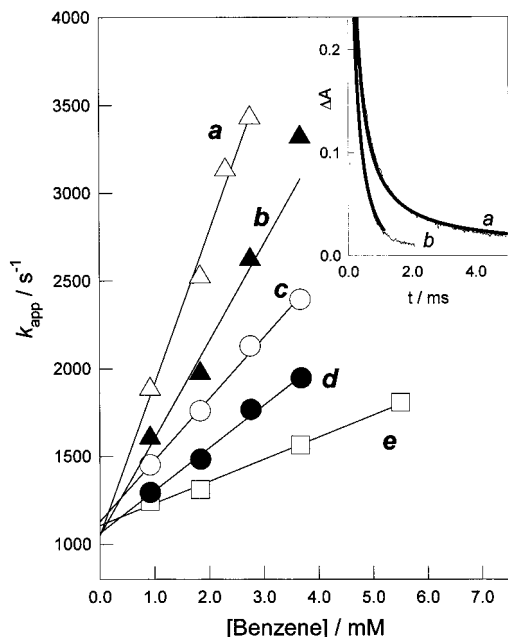


Figure 3. Linear dependence of the first-order decay component (k_{app}) of Cl_2^* on $[\text{Bz}]$ for experiments with (a) $[\text{Cl}^-] = 0.1 \text{ M}$, (b) 0.16 M , (c) 0.24 M , (d) 0.4 M , (e) and 0.5 M , respectively. Inset: Signals obtained at $\lambda_{\text{anal}} = 340 \text{ nm}$ by conventional flash photolysis experiments with $5 \times 10^{-3} \text{ M}$ $\text{K}_2\text{S}_2\text{O}_8$ and 0.1 M NaCl solutions in the absence (upper trace) and in the presence of $2.4 \times 10^{-3} \text{ M}$ benzene (lower trace). The solid lines represent computer simulations (refer to text).

and further reactions involving the latter two species.^{23c} When considerable dispersion in the rate constants is reported, only those values supported by detailed experimental methods were considered, as depicted in Table 1. The computer program does not assume a priori equilibrium conditions for any of the reversible reactions, as such an operation would limit our analysis to particular sets of equilibrium conditions.

Formation of intermediate $(\text{HOClH})^*$ in the reactions of water with Cl_2^* and Cl^* (reactions 7 and 8, respectively) and the reverse reaction 9, with $k_9 \leq 10^3 \text{ s}^{-1}$ was proposed by McElroy² in order to account for the experimentally observed dependence of the Cl_2^* decay on pH. Deprotonation of $(\text{HOClH})^*$ radicals to ClOH^* (reaction 10), its reverse reaction 11, and the subsequent reversible decomposition of ClOH^* to OH^* and Cl^- (reactions 12 and 13) are in agreement with the reactions proposed by Jayson for the formation of Cl_2^* by HO^* and Cl^- .³ The diffusion-controlled reaction between $(\text{HOClH})^*$ and Cl^- , reaction 14, was also proposed in ref 2 in order to account for the observed rate of Cl_2^* formation in pulse radiolysis experiments of acidic NaCl solutions.³ Though not well documented, this latter reaction has been taken into account in this work since, otherwise, simulated profiles differed considerably from experimental results. Simulations showed that the recombination of Cl^* atoms is not significant under our experimental conditions, and consequently, this reaction has been neglected.

Cl_2^* , Cl^* , and $\text{Cl}_2/\text{Cl}_3^-$ are the main species showing absorption at 340 nm. Simulated concentration profiles for Cl_2^* , Cl^* , and $\text{Cl}_2/\text{Cl}_3^-$ were converted into the corresponding absorbance profiles taking $\epsilon(\text{Cl}_2^*) = 9600 \text{ M}^{-1} \text{ cm}^{-1}$,^{7,19} $\epsilon(\text{Cl}^*) = 3800 \text{ M}^{-1} \text{ cm}^{-1}$,²⁴ $\epsilon(\text{Cl}_2) = (68 \pm 5) \text{ M}^{-1} \text{ cm}^{-1}$,²⁵ and $\epsilon(\text{Cl}_3^-) = (178 \pm 5) \text{ M}^{-1} \text{ cm}^{-1}$.²⁵ The simulations show that Cl^* contribution to the absorption profiles at 340 nm is negligible, in agreement with our previous assumptions.

For $k_9 = 5 \times 10^4 \text{ s}^{-1}$ and $k_{14} = 8 \times 10^9 \text{ s}^{-1} \text{ M}^{-1}$, excellent agreement between experimental and simulated data is obtained,

TABLE 2: Manifold of Reactions of Cl^* and Cl_2^* to Be Considered in the Presence of Benzene

	$k/\text{M}^{-1} \text{ s}^{-1}$	
$\text{Cl}_2^* + \text{Bz} \rightarrow \text{Cl}^- +$	$< 1 \times 10^5$ ^a	(20)
organic radicals		
$\text{Cl}^* + \text{Bz} \rightarrow$	$6 \times 10^9 \leq k_{21} \leq 1.2 \times 10^{10}$ ^b	(21)
organic radicals (R^*)		
$\text{Cl}_2^* + \text{R}^* \rightarrow$	c	(22)
products		
$\text{Bz} + \text{HO}^* \rightarrow$	7.8×10^9 ^d	(23)
HCHD		
$\text{Bz} + \text{SO}_4^{\bullet-} \rightarrow$	3×10^9 ^e	(24)
HCHD		
$\text{R}^* + \text{R}^* \rightarrow$	$(1.4 \pm 0.4) \times 10^9$ ^c	(25)
$\text{R}^* \rightarrow \text{Cl}^* + \text{Bz}$	$< 10^4 \text{ s}^{-1}$ ^c	(-21)

^a This work. ^b This work. The upper limit is estimated for $k_{22} < 1 \times 10^9 \text{ M}^{-1} \text{ s}^{-1}$, and the lower limit for $k_{22} > 5 \times 10^9 \text{ M}^{-1} \text{ s}^{-1}$, see text. ^c See text. ^d Reference 32. ^e Reference 26.

both for laser and conventional flash photolysis experiments with $1 \times 10^{-4} \text{ M} < [\text{Cl}^-] < 0.6 \text{ M}$, as shown by the solid traces in Figure 1. We may therefore deduce that the set of reactions depicted in Table 1 may account for the experimental Cl_2^* decay. According to the proposed mechanism, the observed final absorption of a long-lived species is related to the formation of Cl_2 and Cl_3^- (reaction 5). Chlorine hydrolysis to ClOH and HCl in aqueous solutions ($\tau \approx 100 \text{ ms}$, reaction 15) is too slow to affect the Cl_2^* decay.

Dependence of the Cl_2^* Radical Ion Decay Kinetics on the Presence of Benzene. *Experiments with Benzene Concentrations ($[\text{Bz}] < 5 \times 10^{-3} \text{ M}$).* Photolysis of air-saturated aqueous solutions of peroxodisulfate solutions containing chloride ions in the range $0.1 \text{ M} < [\text{Cl}^-] < 0.6 \text{ M}$ and $[\text{Bz}] < 5 \times 10^{-3} \text{ M}$, lead to the formation of transient species with an absorption maximum at 340 nm. The transient spectrum agrees with that of the Cl_2^* radical ion obtained in the absence of benzene and is, therefore, assigned to this species.

For given $[\text{Cl}^-]$, faster decay rates of Cl_2^* are observed by addition of increasing $[\text{Bz}]$, as shown in Figure 3 (inset). The experimental absorption traces at a given wavelength of analysis, $A(\lambda)$, could be fitted according to eq 4. The wavelength-independent constant g depends linearly on $[\text{Bz}]$ (Figure 3) and is related to the first-order decay rate of Cl_2^* . The remaining absorption (term $h(\lambda)$) may be associated with a longer lived species formed after Cl_2^* depletion. $h(\lambda)$ is less than 10% of the initial absorption of Cl_2^* (preexponential factor $f(\lambda)$) and could not be accurately determined from these fittings.

$$A(\lambda) = f(\lambda)e^{-gt} + h(\lambda) \quad (4)$$

Cl^* and Cl_2^* radicals are strong oxidants able to react with many organic compounds. The effect of benzene on the decay rate of Cl_2^* can be understood, if reactions 20 and 21 (Table 2) efficiently compete with the decay reactions of Cl_2^* and Cl^* depicted in Table 1.

The total concentration of the organic radicals R^* formed from the reaction of benzene with Cl^* and Cl_2^* cannot exceed $[\text{SO}_4^{\bullet-}]_0$, therefore, $[\text{R}^*] \leq 3 \times 10^{-5} \text{ M}$ (vide supra). Consequently, a diffusion-controlled reaction between R^* and Cl_2^* , reaction 22, may accelerate the decay kinetics of Cl_2^* radical ions, but in a first approximation, this contribution of reaction 22 will not be considered.

The efficient removal of HO^* radicals in the presence of benzene, reaction 23, does not allow the establishment of equilibrium conditions in eq1, and reactions of Cl_2^* and Cl^* with water may be considered as simple first-order reactions.

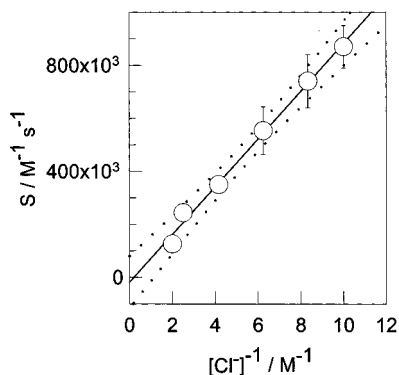


Figure 4. Plot of the slopes (S) of the straight lines shown in Figure 3 vs $[\text{Cl}^-]^{-1}$. The dotted line shows the 99% confidence interval for a linear regression.

TABLE 3: Intercepts of the Plots of k_{app} vs Benzene Concentration Obtained for Different Values of $[\text{Cl}^-]$

$[\text{Cl}^-]/\text{M}$	intercept/ s^{-1}
0.10	1050 ± 160
0.12	1275 ± 120
0.16	1055 ± 180
0.24	1130 ± 40
0.40	1065 ± 40
0.50	1110 ± 30

If reactions 3, 4, 7, 8, 20, and 21 are the main reactions depleting $\text{Cl}_2^{\bullet-}$, which is assumed in equilibrium with Cl^{\bullet} , and considering $K_{3,4}[\text{Cl}^-] > 1$, the apparent first-order decay rate constant of $\text{Cl}_2^{\bullet-}$, k_{app} , is given by eq 5.

$$k_{\text{app}} = k_7 + \frac{k_8}{K_{3,4}[\text{Cl}^-]} + \left[\frac{k_{21}}{K_{3,4}[\text{Cl}^-]} + k_{20} \right] [\text{Bz}] \quad (5)$$

In fact, plots of k_{app} vs $[\text{Bz}]$ (Figure 3) fit to eq 5. However, for the Cl^- concentration range used in these experiments, reaction 8 does not contribute to the first-order decay component of $\text{Cl}_2^{\bullet-}$ as $(k_8/K_{3,4}[\text{Cl}^-]) \ll k_7$. The intercept values for the straight lines as those shown in Figure 3 are depicted in Table 3. As, within the experimental error, these values are independent of the chloride ion concentration, the average value $1115 \pm 140 \text{ s}^{-1}$ ³⁸ is a good estimation for k_7 , in agreement with previous reported values.⁷ The slopes of the curves as those shown in Figure 3 depend on $[\text{Cl}^-]^{-1}$ as expected from eq 5 and shown in Figure 4.

From the slope of the linear function in Figure 4, the bimolecular rate constant $k_{21} = (1.2 \pm 0.6) \times 10^{10} \text{ M}^{-1} \text{ s}^{-1}$ is obtained. The observed negligible value for the intercept yields $k_{20} < 1 \times 10^5 \text{ M}^{-1} \text{ s}^{-1}$ within the limits of experimental error.

To evaluate the contribution of reaction 22 to the concentration profiles of $\text{Cl}_2^{\bullet-}$, a detailed kinetic analysis was performed with the aid of computer simulations. For this purpose, the set of reactions depicted in Table 1 along with reactions 20–24 in Table 2, was used to fit typical experiments, as that shown in Figure 3 (inset).

Simulated and experimental profiles show excellent agreement when the k_{20} and k_{21} values retrieved from the kinetic analysis already described are used, and for $k_{22} < 10^9 \text{ M}^{-1} \text{ s}^{-1}$. Despite that $k_{20} < 10^5 \text{ M}^{-1} \text{ s}^{-1}$ from the simplified analysis, the simulation program shows that reaction 20 does not contribute to the $\text{Cl}_2^{\bullet-}$ decay already for $k_{20} \leq 10^6 \text{ M}^{-1} \text{ s}^{-1}$. For higher input values of k_{22} , simulated decays are faster than experimental ones. Assuming $k_{22} > 5 \times 10^9 \text{ M}^{-1} \text{ s}^{-1}$, a value $k_{21} = 6 \times 10^9 \text{ M}^{-1} \text{ s}^{-1}$ is required for an agreement between simulated and

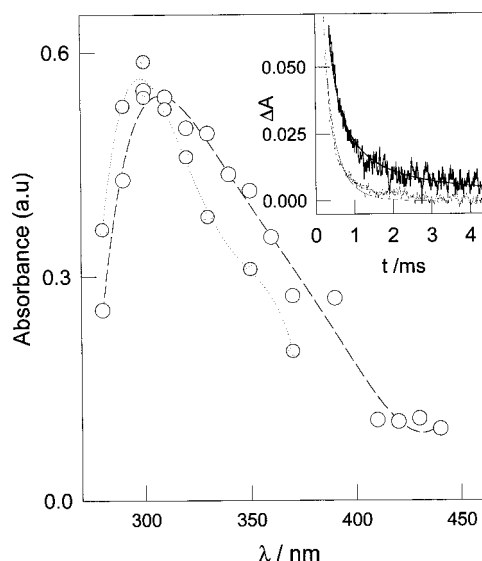


Figure 5. Absorption spectrum of the organic transients obtained (O) 20 μs and (●) 400 μs after irradiation with Nd:YAG laser and conventional flash lamp, respectively, of nitrogen-saturated $5 \times 10^{-3} \text{ M}$ solutions of $\text{K}_2\text{S}_2\text{O}_8$ and 0.1 M of NaCl in the presence of benzene ($> 1 \times 10^{-2} \text{ M}$). Inset: Transient absorption profiles at 300 nm obtained from (a) N_2 and (b) air-saturated solutions containing $5 \times 10^{-3} \text{ M}$ $\text{K}_2\text{S}_2\text{O}_8$, 0.1 M of NaCl, and $2 \times 10^{-2} \text{ M}$ of benzene. The solid lines represent computer simulations (refer to text).

experimental profiles, as shown by the solid traces in Figure 3 (inset). Reactions of Cl^{\bullet} atoms with the organic radicals R^{\bullet} show a negligible effect on the simulated decays, even assuming diffusion controlled rate constants, and were therefore not taken into account.

A value $k_{22} \geq 5 \times 10^9 \text{ M}^{-1} \text{ s}^{-1}$ may be realistic, since reported reactions between $\text{Cl}_2^{\bullet-}$ and radicals such as ClO_2^{\bullet} and HO_2^{\bullet} are of that order of magnitude.²⁶ The value $k_{21} = 6 \times 10^9 \text{ M}^{-1} \text{ s}^{-1}$ is in complete agreement with that reported for the reaction in benzene as solvent.¹² A very low reactivity of $\text{Cl}_2^{\bullet-}$ toward benzene is also in agreement with the reported rate constants for its reactions with most organic substrates.^{5,7,27}

Experiments with $[\text{Bz}] > 10^{-2} \text{ M}$. For irradiation experiments with $[\text{Cl}^-] = 0.1 \text{ M}$ and $[\text{Bz}] \geq 1 \times 10^{-2} \text{ M}$, reaction 21 is very efficient and $\text{Cl}_2^{\bullet-}/\text{Cl}^{\bullet}$ radicals are readily scavenged. Under these experimental conditions, a lifetime $\tau < 60 \mu\text{s}$ is expected for $\text{Cl}_2^{\bullet-}$ and observed in laser flash photolysis experiments. At longer times of analysis, formation of transient species absorbing in the wavelength region from 290 to 360 nm with a maximum at approximately 300–310 nm was observed. The transient spectrum observed 20 μs after the laser shot agrees, within experimental error, with that observed in conventional flash experiments at times up to fractions of milliseconds, as shown in Figure 5. Blank experiments performed with benzene solutions under identical experimental conditions but in the absence of $\text{S}_2\text{O}_8^{2-}$ showed no signal, indicating that any contribution of benzene photolysis is negligible and that the observed transients are mainly formed after reaction 21.

The absorption coefficient of the transient is estimated from laser experiments performed with N_2 -saturated solutions in the presence and absence of benzene. Under otherwise identical experimental conditions, it may be assumed that the same amount of $\text{Cl}_2^{\bullet-}$ is formed in all the experiments and mainly consumed by reaction 21. The estimated absorption coefficient would be a lower limit value if this latter condition does not apply. Taking $\epsilon(\text{Cl}_2^{\bullet-}, 340 \text{ nm}) = 9600 \text{ M}^{-1} \text{ cm}^{-1}$,^{7,19} the $\text{Cl}_2^{\bullet-}$ concentration formed in a typical experiment as shown in Figure

le is $\approx(1.45 \pm 0.1) \times 10^{-6}$ M (also in complete agreement with $[\text{SO}_4^{\bullet-}]_0$, vide supra). Thus, a value of $\epsilon(300 \text{ nm}) = 2800 \pm 500 \text{ M}^{-1} \text{ cm}^{-1}$ is obtained for the organic transient.

The experimental traces obtained at a given wavelength of analysis λ from conventional flash photolysis experiments with nitrogen saturated solutions (Figure 5 inset) may be well fitted to a second-order law. The second-order rate constants are insensitive to $[\text{S}_2\text{O}_8^{2-}]$ and $[\text{Bz}]$ in the range of $[\text{Bz}] \geq 1 \times 10^{-2}$ M and may be associated with the recombination of the organic radicals (reaction 25). For the optical path length $l = 11$ cm and $\epsilon(300 \text{ nm}) = 2800 \pm 500 \text{ M}^{-1} \text{ cm}^{-1}$, the rate constant $2k_{25} = (1.4 \pm 0.4) \times 10^9 \text{ M}^{-1} \text{ s}^{-1}$ is calculated.

A transient absorbing at 490 nm with a lifetime of 1–10 μs , which has been attributed to the π complex,^{12,14} is not observed in our laser experiments. We may therefore conclude that a π complex between benzene and Cl^\bullet atoms is either not formed or decomposes in aqueous solutions in less than 50 ns to yield a secondary organic radical with an absorption maximum at approximately 300 nm.

Hydroxycyclohexadienyl radicals (HCHD) are known to present a single absorption maximum at 300–310 nm^{28,29} with an absorption coefficient $\geq 2000 \text{ M}^{-1} \text{ cm}^{-1}$. The bimolecular decay rates $2k_{25}/\epsilon_{\text{max}}$ are in the range from $(1-5) \times 10^5 \text{ s}^{-1} \text{ cm}^{-1}$ for a wide number of substituted HCHD.²⁸⁻³³ The observed transient showing absorption and kinetic properties very similar to those of HCHD is assumed to represent the Cl-CHD radical, in agreement with the postulated structure of the corresponding σ complex. In fact, the absorption spectra of CHD radicals of 3-chlorotoluene formed upon addition of H atoms and those formed upon addition of HO^\bullet radicals are very similar.^{28c}

HCHD radicals reversibly react with molecular oxygen yielding peroxy radicals (PR), reaction 26, which typically exhibit broad absorption only at $\lambda < 300 \text{ nm}$.^{30,31}



Experiments performed under identical conditions but in the presence of molecular oxygen show the same transient spectrum, although with lower absorbance and faster depletion rates (Figure 5 (inset)). Experimental traces obtained for air-saturated solutions could be well-fitted to a first-order law. The high absorption of the solutions below 280 nm precluded time-resolved detection at shorter wavelengths, and, consequently, PR formation cannot be observed. However, the lower concentration of Cl-CHD and its faster decay kinetics in the presence of molecular oxygen may be rationalized by the existence of a reversible reaction between Cl-CHD radicals and O_2 , similar to reaction 26. An equilibrium constant $K_{26} = 1100 \pm 500 \text{ M}^{-1}$ is estimated from conventional flash experiments performed with N_2 , O_2 , and air-saturated solutions under otherwise identical experimental conditions, assuming that identical initial concentrations of radicals are formed in all the experiments and that equilibrium conditions for reaction 26 are established.

Reported data concerning the equilibrium constants K_{26} of several HCHD radicals show that the equilibrium shifts away from the peroxy radicals with increasing electron-withdrawing power of the substituent, indicating that a considerable electron-density at open-shell carbon is required for the formation of a C– O_2 bond. Cl being a stronger electron-withdrawing group than HO, it may be expected that the reaction of O_2 with Cl-CHD radicals is less favorable than that with the parent HCHD radical. In fact, the presence of a Cl substituent in the HCHD radical of benzene lowers the equilibrium constant from $2.6 \times$

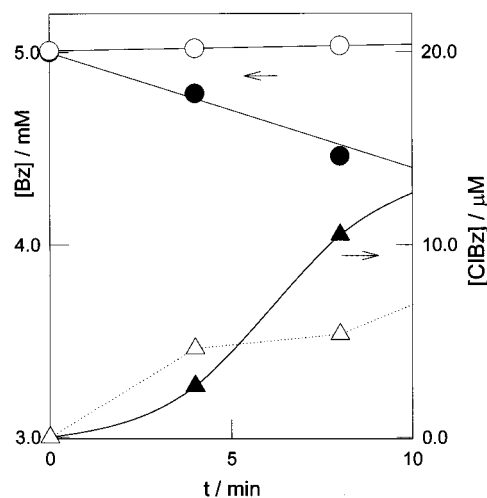


Figure 6. Depletion of (●) $[\text{Bz}]$ and evolution of (▲) [chlorobenzene] and 2,4-hexadiene-aldehyde (△, arbitrary units) vs irradiation time for preparative experiments performed with air saturated aqueous solutions containing 1×10^{-4} M of $\text{K}_2\text{S}_2\text{O}_8$, 0.5 M of NaCl, and 5×10^{-3} M of benzene. Depletion of (○) $[\text{Bz}]$ in blank experiments performed in the absence of $\text{K}_2\text{S}_2\text{O}_8$.

10^4 M^{-1} ^{31b} to $0.5 \times 10^4 \text{ M}^{-1}$.^{31a} The value of K_{26} found for the Cl-CHD radical is on the order of the one reported for the HCHD radical of chlorobenzene.

To test the presence of reaction 26, the experimental traces were simulated. An adequate set of reactions includes equilibrium 26, recombination of Cl-CHD (reaction 25), recombination of PR radicals, and a first-order decay of PR.³⁰ This simulation shows that the decay of Cl-CHD radicals in air- and oxygen-saturated solutions is not sensitive to the input values concerning the recombination of PR radicals. Due to equilibrium (26), the depletion rate of Cl-CHD is controlled by the first-order decay of PR under our experimental conditions for oxygen- and air-saturated solutions. A good agreement between experimental and simulated profiles (Figure 5 (inset)) is obtained for $k = 1.4 \times 10^4 \text{ s}^{-1}$, where k is the mono-molecular decay rate constant of PR which is of the order reported for the decomposition of many alkyl peroxy radicals.³⁴

Product Analysis. Identification of the products formed after the reactions of $\text{Cl}_2^{\bullet-}/\text{Cl}^\bullet$ with benzene in air-saturated solutions was performed with photolysis experiments using immersion-type reactors. The photolysis of air-saturated aqueous solutions of benzene (2×10^{-2} M) yielding oxidation products, such as phenol, catechol, dihydrocatechol, and benzoquinone, required experimental conditions designed to minimize benzene photolysis. High $[\text{Cl}^-]/[\text{S}_2\text{O}_8^{2-}]$ ratios avoid oxidation of benzene by sulfate radicals, reaction 24.

Irradiation of aqueous solutions containing $[\text{Bz}] = 5 \times 10^{-3}$ M, $[\text{S}_2\text{O}_8^{2-}] = 1 \times 10^{-4}$ M, and $[\text{Cl}^-] = 0.5$ M showed depletion of benzene and the simultaneous formation of two main products identified as chlorobenzene and 2,4-hexadiene-aldehyde by GC/MS (Figure 6). Experiments with increasing concentrations of benzene showed higher yields of chlorobenzene. Diminution of the concentration of dissolved molecular oxygen is also observed.

Because chlorobenzene represented less than 10% of the consumed benzene, we deduce that oxidation yielding aliphatic species must be the major route of the reaction of benzene with Cl^\bullet in air saturated aqueous solutions. Aliphatic C_1 to C_4 products could not be analyzed and identified, because they elute with the solvent under the given analytical conditions.

Conclusions

The understanding of the complex aqueous phase chemistry of the $\text{Cl}_2^{\bullet-}/\text{Cl}^{\bullet}$ couple is relevance to discerning the fate of oxidizing radicals in cloudwater droplets containing significant concentrations of chloride ions and is a prerequisite for a detailed investigation of their reactivity toward organic substrates. With the reaction sequences depicted in Table 1, purely second-order, largely first-order and mixed first- and second-order decays of $\text{Cl}_2^{\bullet-}$, observed for different $[\text{Cl}_2^{\bullet-}]$ to $[\text{Cl}^{\bullet}]$ ratios, may be simulated. According to the proposed mechanism, reactions of $\text{Cl}_2^{\bullet-}$ and Cl^{\bullet} with water (reactions 7 and 8, respectively) efficiently lead to the formation of HO^{\bullet} radicals for $[\text{Cl}^{\bullet}] < 10^{-2}$ M, where the condition $v_{14} < v_{10}$ applies. Therefore, in marine clouds containing $[\text{Cl}^{\bullet}] \approx 0.5$ mM, reactions 7 and 8 will lead to an increasing oxidation capacity of the aqueous medium. Under conditions of $[\text{Cl}^{\bullet}] \approx 0.5$ mM and low radical concentrations, $\text{Cl}_2^{\bullet-}$ lifetime is expected to be of the order of fractions of milliseconds, and $\text{Cl}_2^{\bullet-}$ may thus react with organic constituents of the aqueous troposphere. Chlorine atoms concentrations are less important. However, due to the reversibility of reaction 3 and their high reactivity (vide infra), Cl^{\bullet} reactions with organic substrates may constitute an important sink for $\text{Cl}_2^{\bullet-}$ radical ions, if organic constituents are present in concentrations higher than 10^{-5} M.

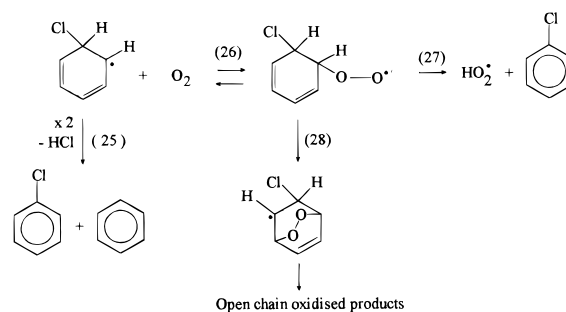
We found that Cl^{\bullet} atoms are much more reactive toward benzene ($6 \times 10^9 \text{ M}^{-1} \text{ s}^{-1} \leq k_{21} \leq 1.2 \times 10^{10} \text{ M}^{-1} \text{ s}^{-1}$) than $\text{Cl}_2^{\bullet-}$ radical ions ($k_{20} < 1 \times 10^5 \text{ M}^{-1} \text{ s}^{-1}$). This observation is in agreement with studies involving aliphatic organic compounds reported by Gilbert¹⁰ and Buxton.¹⁹ Reaction of Cl^{\bullet} atoms with benzene proceeds via $\text{C}_6\text{H}_6\text{-Cl}$ adduct formation, probably best represented as a Cl-CHD radical. We were unable to observe any stable π adduct between Cl^{\bullet} atoms and C_6H_6 . Reported calculations on such a π complex estimate very low bond energies (< 12 kJ),¹⁶ suggesting that, unless highly stabilized by the solvent, it cannot survive more than a few picoseconds at room temperature and, consequently, is too short-lived to play any role in a sequence of chemical reactions.

H atom abstraction from the aromatic ring yielding reactive phenyl radicals would be another possible reaction pathway. Phenyl radicals readily react (half-life $< 3 \mu\text{s}$ in air saturated solutions) with molecular oxygen to yield aryl peroxy radicals absorbing in the spectral domain of 400–500 nm.³⁵ Such peroxy radicals decay by bimolecular recombination with rate constants $< 10^7 \text{ M}^{-1} \text{ s}^{-1}$,^{35b} and consequently, could be detected with our experimental setup. The absence of traces absorbing in the wavelength range of 400–500 nm does not support an important participation of such reactions.

Like the hydroxyl radical, the reaction of Cl^{\bullet} with aromatics involves addition to the ring rather than hydrogen abstraction.³⁶ Halogenation and radiation-induced hydroxylation of substituted benzenes have been suggested to be similar in nature, as both reacting species are electrophiles. The Hammett ρ values reported for aromatic chlorination and hydroxylation (-0.56 and -0.52 , respectively) as well as the relative distribution of radical addition are comparable.^{28c} Formation of π complexes between the electrophilic HO^{\bullet} and the π electrons of aromatic systems with diffusion-controlled rates, irrespective of the substituents at the aromatic ring, has been proposed as a precursor of a σ complex shown as HCHD radicals.³⁶ Rearrangement from the π to σ complex takes place in the nanosecond time range.

The significant difference between gas and aqueous phase reactions of Cl atoms and benzene is that in our experiments in aqueous solutions there is no evidence for H-atom abstraction from the aromatic ring nor for dissociation of Cl-CHD (reaction

SCHEME 1



(-21)). A possible explanation for the apparent mechanistic differences is that Cl-CHD is always formed in each phase but it does not significantly dissociate on the time scale of our observations. Under the experimental conditions attained in our time-resolved experiments, Cl-CHD scavenging by $\text{Cl}_2^{\bullet-}$ (reaction 2) may be sufficiently fast to prevent dissociation, thus $v_{22} > v_{-21}$ and reactions 21 and -21 are not equilibrated. Taking $k_{22} > 5 \times 10^9 \text{ M}^{-1} \text{ s}^{-1}$ and $[\text{Cl}_2^{\bullet-}] \approx 10^{-6}$ M, $k_{-21} < 10^4 \text{ s}^{-1}$ is estimated. From the gas-phase data¹⁶ it can be estimated that reaction (-21) would have a half-life of ca. $0.2 \mu\text{s}$ which is significantly shorter than that estimated in aqueous solutions. These observations indicate that the role of the aqueous medium is that of stabilizing the Cl-CHD radicals. A similar behavior was reported for the HCHD radical lifetimes in the gas and aqueous phase.³⁶

The rate constant for H abstraction in the gas phase is $7.8 \times 10^4 \text{ M}^{-1} \text{ s}^{-1}$.¹⁶ Assuming a similar value in aqueous media, the competition of this reaction with the efficient Cl-CHD formation is of no significance, as reaction -21 is also irrelevant.

Reaction of Cl-CHD with O_2 has been proposed to yield chlorobenzene and HO_2^{\bullet} radicals, reaction 27 in Scheme 1.^{13a} However, chlorobenzene is found to be a minor product (molar yield $< 10\%$) in preparative experiments performed with air-saturated solutions. This result is an indication that the reaction of Cl-CHD with O_2 proceeds via more than one reaction channel, as already observed in the gas phase.¹⁶ In analogy to the reactions leading to aliphatic oxidation products from hydroxycyclohexadienylperoxy radicals,^{31b} reaction 28 may compete with HO_2^{\bullet} elimination. At the present state of knowledge, the formation of 2, 4-hexadiene-aldehyde from Cl-CHD radicals cannot be explained. Subsequent reactions of the peroxy radical formed by the addition of molecular oxygen to Cl-CHD seem to be rather complex and have not yet been investigated in detail.¹⁶

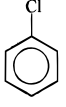
Cl-CHD recombination, reaction 25, leads to chlorobenzene formation and may contribute to the decay of Cl-CHD radicals in air-saturated solutions (vide supra). This reaction is certainly less significant in steady-state experiments, where only very low radical concentrations are obtained. Biphenyl products were not detected (detection limit: $0.1 \mu\text{M}$).

Experimental Section

Materials. Potassium peroxodisulfate (Riedel de Haën), sodium chloride (Merck p.a.), and benzene (Merck p.a.) were used as received. Distilled water was obtained from a Millipore system ($> 18 \Omega \text{ cm}^{-1}$, < 20 ppb of organic carbon).

Time-Resolved Experiments. Flash-photolysis experiments were carried out using conventional equipment (Xenon Co. model 720C) with modified optics and electronics (ref 23 and references therein). The emission of the flash lamps was filtered with a saturated solution of benzene in water, to minimize

TABLE 4: Mass Spectra and Probable Structures of Detected Products

	(RT 7.05) 114 ($[M+2]^+$, 32.0); 113($[M+1]^+$, 8.0); 112(M^+ , 100.0); 77($[C_6H_5]^+$, 53.0); 51($[C_6H_3]^+$, 30.0); 50($[C_6H_2]^+$, 20.0); 39($[C_6H_3]^+$, 30.0).
H(O)C-[HC=CH] ₂ -CH ₃	(RT 7.00) 96 (M^+ , 32.0); 95 ($[95-H]^+$, 100.0); 81 ($[HC=C-CH=CH-C(O)H_2]^+$, 20.7); 77 ($[96-H_2O-H]^+$, 38.7); 67($[95-CO]^+$, 42.5); 66 ($[96-H_2CO]^+$, 19.8); 55 ($[HC(O)-CH=CH]^+$, 7.1); 53 ($[H_3C-CH=C=CH]^+$, 11.3); 51 ($[HC=CH-C=CH]^+$, 9.4); 41 ($[H_3C-CH=CH]^+$, 11.3); 39 ($[41-H_2]^+$, 15.0); 29 ($[C(O)H]^+$, 2.8); 27 ($[H_2C=CH]^+$, 4.7).

benzene photolysis in the reaction system. The optical path length of the reaction cell / is either 11 or 20 cm. Laser experiments were performed with a Spectron SL400 Nd:YAG system generating 266 nm pulses (~8 ns pulse width). The laser beam was defocalized in order to cover the entire path length (1 cm) of the analyzing beam produced by a 150 W Xe Lamp. The experiments were performed with a quartz cell in a 90° geometry. The detection system comprised a PTI monochromator coupled to a Hamamatsu R666 PM tube. The signal was acquired by a digitizing scope (Hewlett-Packard 54504), where it was averaged and transferred to a computer.

Preparative Experiments. A cylindrical low-pressure Hg lamp (Heraeus, MNMI 35/20, Germany) emitting at 254 nm and presenting much lower emissions at $\lambda > 312$ nm was used. The photochemical reactor was of annular geometry (volume: 400 mL) adapted for the lamp which was immersed within a quartz tube. The annular optical path in the reactor was of the order of 1 cm. The whole reactor was immersed in a thermostat controlling the temperature at 25 ± 1 °C.

Methods. Unless otherwise indicated, typical $S_2O_8^{2-}$ concentrations were 5.0×10^{-3} M for conventional flash photolysis and 2.0×10^{-2} M for laser experiments. The pH of the peroxodisulfate solutions was approximately 3.0 to 2.05 due to the acid content incorporated with the $K_2S_2O_8$, containing water and acid as impurities.³⁷ Addition of buffers was avoided, since their components may react with $SO_4^{\cdot-}$ radical ions.³⁴ The ionic strength of the solutions was within the range of 0.005–0.2 M.

Solutions of benzene were prepared by dilution of a saturated aqueous solution at 25 °C. For experiments performed in the absence of molecular oxygen, the benzene-saturated aqueous solutions and the water used for dilution were bubbled with N_2 or Ar. The concentrations of benzene and chloride ions used in all experiments fulfilled the condition that reaction of benzene with sulfate radicals can be neglected.

Organic products were extracted from the aqueous solutions with a fixed volume of chloroform and the extracts stored in glass vials with PTFE/silicone septum-lined screw caps and minimized headspace. Analysis of the extracts was performed by gas chromatography with a HP 6890 chromatograph equipped with a fused silica HP5-MS GC capillary column and coupled to an HP 5973 mass selective detector. The analysis was performed by using a temperature program starting at 80 °C and ending at 200 °C at a rate of 10 °C/min and held at 200 °C for 5 min. Helium was used as carrier gas with a flow rate of 29 cm³/s. Injection volumes were of 20 μ L.

Mass spectra and probable structures of detected products are shown in Table 4. The pH of the samples was periodically controlled with a Methrom-Herisau pH meter model E512. The

concentration of dissolved oxygen in the samples was determined with a specific oxygen electrode (Orion 97-0899).

Acknowledgment. We thank Dr. G. Carrillo Leroux from the Faculty of Engineering, University of Sao Paulo (Brazil), for doing the simulations with the stiff solver program. This research was supported by Fundación Antorchas, Consejo Nacional de Investigaciones Científicas y Técnicas, Argentina (CONICET), Comisión de Investigaciones Científicas de la Provincia de Buenos Aires (CIC), and the Deutsche Akademische Austauschdienst (DAAD). J.A.R. thanks CONICET for a graduate studentship. D.O.M. is a research member of CIC, S.G.B. and M.C.G. are research members of CONICET.

References and Notes

- (1) (a) Walcek, C.; Yuan, H. H.; Stockwell, W. R. *Atmos. Environ.* **1997**, *31*, 1221. (b) Jacob, D. J. *J. Geophys. Res.* **1986**, *91*, 9807. (c) Abbatt, J. P. D.; Waschewsky, G. C. G. *J. Phys. Chem.* **1998**, *102*, 3719.
- (2) McElroy, W. J. *J. Phys. Chem.* **1990**, *94*, 2435.
- (3) Jayson, G. G.; Parsons, B. J.; Swallow, A. J. *J. Chem. Soc., Faraday Trans.* **1973**, *69*, 1597.
- (4) Jacobi, H. W.; Herrmann, H.; Zellner, R. *Ber. Bunsen-Ges. Chem.* **1997**, *101*, 1909.
- (5) Hasegawa, K.; Neta, P. *J. Phys. Chem.* **1978**, *82*, 854.
- (6) Wagner, I.; Karthäuser, J.; Strehlow, H. *Ber. Bunsen-Ges. Chem.* **1986**, *90*, 861.
- (7) (a) Buxton, G. V.; Bydder, M.; Salmon, G. A. *J. Chem. Soc., Faraday Trans.* **1998**, *94*, 653. (b) Buxton, G. V.; Bydder, M.; Salmon, G. A. *Phys. Chem. Chem. Phys.* **1999**, *1*, 269.
- (8) (a) Beitz, T.; Bechmann, W.; Mitzner, R. *J. Phys. Chem.* **1998**, *102*, 6766. (b) de Violet, P. F. *Rev. Chem. Intermed.* **1981**, *4*, 121.
- (9) Steenken, S. In *Free Radicals: Chemistry, Pathology and Medicine*; Rice-Evans, C., Ed.; Dormandy T. Richelieu Press: London, 1988; p 51.
- (10) Gilbert, B. C.; Stell, J. K.; Peet, W. J.; Radford, K. *J. Chem. Soc., Faraday Trans. 1* **1988**, *84*, 3319.
- (11) Platz, J.; Nielsen, O. J.; Wallington, T. J.; Ball, J. C.; Hurley, M. D.; Strascia, A. M.; Schneider, W. F.; Sehested, J. *J. Phys. Chem.* **1998**, *102*, 7964.
- (12) Bunce, N. J.; Ingold, K. U.; Landers, J. P.; Luszyk, J.; Scaiano, J. C. *J. Am. Chem. Soc.* **1985**, *107*, 5464.
- (13) (a) Skell, P. S.; Baxter, H. N.; Tanko, J. M.; Chebolu, V. *J. Am. Chem. Soc.* **1986**, *108*, 6300. (b) Chatauneuf, J. E. *Chem. Commun.* **1998**, 2099.
- (14) (a) Bühler, R. E. *Radiat. Res. Rev.* **1972**, *4*, 233 and references therein. (b) Bühler, R. E.; Bossy, J. M. *Int. J. Radiat. Phys. Chem.* **1974**, *6*, 95.
- (15) Raner, K. D.; Luszyk, J.; Ingold, K. U. *J. Phys. Chem.* **1989**, *93*, 564.
- (16) Sokolov, O.; Hurley, M. D.; Wallington, T. J.; Kaiser, E. W.; Platz, J.; Nielsen, O. J.; Berho, F.; Rayez, M. T.; Lesclaux, R. *J. Phys. Chem.* **1998**, *102*, 10671.
- (17) McElroy, W. J.; Waygood, S. J. *J. Chem. Soc., Faraday Trans.* **1990**, *86*, 2557.
- (18) Choure, S. C.; Bamatraf, M. M. M.; Rao, B. S. M.; Das, R.; Mohan, H.; Mittal, J. P. *J. Phys. Chem. A* **1997**, *101*, 9837. Hug, G. L. *Nat. Stand. Ref. Data Ser. (U.S. Nat. Bur. Stand.)* **1981**, *69*.
- (19) Adams, D. J.; Barlow, S.; Buxton, G. V.; Malone, T.; Salmon, G. A. *J. Chem. Soc., Faraday Trans.* **1995**, *91*, 3303.
- (20) (a) Langmuir, M. E.; Hayon, E. *J. Phys. Chem.* **1967**, *71*, 3803. (b) Wu, D.; Wong, D.; di Bartolo, B. *J. Photochem.* **1980**, *14*, 303.
- (21) Huie, R. E. In *Advanced Series in Physical Chemistry*; Barker, J. R., Ed.; World Scientific: New Jersey, 1995; vol. 3.
- (22) Huie, R. E.; Clifton, C. L. *J. Phys. Chem.* **1990**, *94*, 8561.
- (23) (a) Gonzalez, M. C.; Braun, A. M. *Res. Chem. Intermed.* **1995**, *21*, 837. (b) Hindmarsh, A. C. *ACM SIGNUM Newsletter* **1980**, *15*, 11–19. (c) Mártire, D. O.; Gonzalez, M. C. *Int. J. Chem. Kinet.* **1997**, *29*, 589.
- (24) Nagarajan, V.; Fessenden, R. W. *J. Phys. Chem.* **1985**, *89*, 2330.
- (25) Zimmerman, G.; Strong, F. C. *J. Am. Chem. Soc.* **1956**, *79*, 2063.
- (26) Neta, P.; Huie, R. E.; Ross, A. B. *J. Phys. Chem. Ref. Data* **1988**, *17*, 1146.
- (27) Jacobi, H. W.; Wicktor, F.; Herrmann, H.; Zellner, R. *Int. J. Chem. Kinet.* **1999**, *31*, 169.
- (28) (a) Steenken, S. In *Free Radicals in Synthesis and Biology*. NATO ASI Series C 260; Minisci, F., Ed.; Kluwer Academic Publishers: Dordrecht, 1989; p 220. (b) Merga, G.; Rao, B. S. M.; Mohan, H.; Mittal, J. P. *J. Phys. Chem.* **1994**, *98*, 9158. (c) Mohan, H.; Mudaliar, M.; Aravindakumar,

C. T.; Rao, B. S.; Mittal, J. P. *J. Chem. Soc., Perkin Trans. 2* **1991**, 2, 1387.

(29) (a) Land, E. J.; Ebert, M. *Trans. Faraday Soc.* **1967**, 63, 1181. (b) Draper, P. B.; Fox, M. A.; Pelizzetti, E.; Serpone, N. *J. Phys. Chem.* **1989**, 93, 1938.

(30) Cencione, S. S.; Gonzalez, M. C.; Mártire, D. O. *J. Chem. Soc., Faraday Trans.* **1998**, 94, 2933.

(31) (a) Fang, X.; Pan, X.; Rahmann, A.; Schuchmann, H. P.; von Sonntag, C. *Chem. Eur. J.* **1995**, 1, 423. (b) von Sonntag, C.; Schuchmann, H. P. *Angew. Chem., Int. Ed. Engl.* **1991**, 30, 1229.

(32) Buxton, G. V.; Greenstock, C. L.; Helman, W. P.; Ross, A. B. *J. Phys. Chem. Ref. Data* **1988**, 17, 513.

(33) Mohan, H.; Mittal, J. P. *J. Chem. Soc., Faraday Trans.* **1995**, 91, 2121.

(34) Neta, P.; Huie, R. E.; Ross, A. B. *J. Phys. Chem. Ref. Data* **1990**, 19, 413.

(35) (a) Sommeling, P. M.; Mulder, P.; Louw, R.; Avila, D. V.; Luszyk, J.; Ingold, K. U. *J. Phys. Chem.* **1993**, 97, 8361. (b) Alfasi, Z. B.; Maguet, S.; Neta, P. *J. Phys. Chem.* **1994**, 98, 8019.

(36) Ashton, L.; Buxton, G. V.; Stuart, C. *J. Chem. Soc., Faraday Trans.* **1995**, 91, 1631.

(37) Riedel de Häen (Germany). Personal communication. 1998.

(38) The error bars for the values reported here are in all cases considered for a 99% confidence level.